length of the chains considered in our work. This circumstance and the appreciable simulation uncertainties prevent us from estimating a power law for the ratio. If the N^{-2} scaling would hold for shear flows with HI, the behavior that we observe for our short chains is far from it. Our most noticeable finding is that when the hydrodynamic interaction is included the ratios are remarkably smaller than those obtained in the absence of HI. We even forecast that the scaling law of the ratio with HI could be different than that without HI.

In regard to the second effect that causes the stretching of bead-and-spring chains, it can be detected in the angle α_i, with $i = 2, ..., N-1$, defined as the angle subtended by the directions of bonds $\mathbf{b}_{i-1}$ and $\mathbf{b}_i$. In Table IV we present values for the angle in a trimer and for the central and terminal angles when $N = 8$ and 20. We first note that the for the trimer $\langle \cos \alpha_1 \rangle \simeq 0$ and $\dot{\gamma}$ is as high as 5, a value for which $\langle R^2 \rangle$ is about 50% larger than $\langle R^2 \rangle_0$. Thus it seems that the primary contribution to the elongation of the model chain is the stretching of the springs rather than their alignment. The latter takes place at high shear rates and depends appreciably on N. We have made no attempt to characterize the N dependence of $\langle \cos \alpha_i \rangle$, but we notice from the results in Table IV that the central angles deformed in the shear flow more than the terminal ones and that hydrodynamic interaction effects make the deformation smaller than expected if interaction were absent. Thus our results including hydrodynamic interactions for varying N complement those from other analytical or simulation studies.[15,16]

Acknowledgment. We are grateful to A. Iniesta and F. G. Diaz for their help in many aspects of this work, which was supported by Grant PB87-0694 from the Comisión Interministerial de Ciencia y Tecnologá.

References and Notes

(1) Bird, R. B.; Hassager, O.; Armstrong, R. C.; Curtiss, C. F. Dynamics of Polymeric Liquids. *Kinetic Theory*; Wiley: New York, 1977; Vol. 2.
(2) Diaz, F. G.; García de la Torre, J.; Freire, J. J. *Polymer* **1989**, *30*, 259.
(3) Bird, R. B.; Saab, H. H.; Dotson, P. J.; Fan, X. J. *J. Chem. Phys.* **1983**, *79*, 5729.
(4) Ermak, D. L.; McCammon, J. A. *J. Chem. Phys.* **1978**, *69*, 1352.
(5) Zylka, W.; Öttinger, H. C. *J. Chem. Phys.* **1989**, *90*, 474.
(6) Liu, T. W. *J. Chem. Phys.* **1989**, *90*, 5826.
(7) Díaz, F. G.; Iniesta, A.; García de la Torre, J. *J. Chem. Phys.* **1987**, *87*, 6021.
(8) Iniesta, A.; Garcia de la Torre, J. *J. Chem. Phys.* **1990**, in press.
(9) Öttinger, H. C. *J. Non-Newtonian Fluid Mech.* **1986**, *19*, 357.
(10) Pistoor, N.; Binder, K. *Colloid Polym. Sci.* **1988**, *266*, 132.
(11) Frisch, H. L.; Pistoor, N.; Sariban, A.; Binder, K.; Fesjian, S. *J. Chem. Phys.* **1989**, *89*, 5194.
(12) Lindner, P.; Oberthur, R. C. *Colloid Polym. Sci.* **1988**, *266*, 886.
(13) Keller, A.; Odell, J. A. *Colloid Polym. Sci.* **1985**, *263*, 181.
(14) Rabin, Y. *J. Chem. Phys.* **1988**, *88*, 4014.
(15) Dotson, P. J. *J. Chem. Phys.* **1983**, *79*, 5730.
(16) Öttinger, H. C. *J. Chem. Phys.* **1986**, *84*, 1850.

Estimation of Free Volume for Gaseous Penetrants in Elastomeric Membranes by Monte Carlo Simulations

S. Trohalaki,† L. C. DeBolt,‡ and J. E. Mark*

Department of Chemistry and the Polymer Research Center, The University of Cincinnati, Cincinnati, Ohio 45221-0172

H. L. Frisch

Department of Chemistry, State University of New York at Albany, Albany, New York 12222. *Received March 8, 1989; Revised Manuscript Received July 3, 1989*

ABSTRACT: Theoretical aspects of the diffusion of small molecules in elastomeric polymer membranes are explored using a Monte Carlo simulation to estimate the free volume fraction in two typical siloxane elastomers. The model took into account the specific chemical structure of the polymer through the rotational isomeric state approximation. Calculated results for the two polymers agree semiquantitatively with experimentally determined diffusion coefficients.

Introduction

Membranes have found important industrial applications in the separation of gas mixtures. Such separations through rubbery polymer membranes is controlled by molecular diffusion of the penetrant molecules.[1,2] Fujita[2] has shown that the binary diffusion coefficient D is related to the free volume fraction f by

$$D(T,\phi) = A \exp[-B/f(T,\phi)] \quad (1)$$

where T is the absolute temperature, ϕ is the volume fraction of the penetrant gas, and A and B are constants. Evaluation of a polymer's free volume fraction is therefore useful in predicting its potential for gas separation. One way of doing this is by means of molecular simulations. We restrict our simulations here to siloxanes because they have the highest oxygen permeabilities among rubbery polymers.

† Current address: Department of Chemical Engineering and Materials Science, Syracuse University, Syracuse, NY 13244.
‡ Current address: Sherwin Williams Research Center, 10909 South Cottage Grove Avenue, Chicago, IL 60628.

0024-9297/90/2223-0813$02.50/0

Fujita's model[2] is based on a theory for self-diffusion of a hard-sphere liquid by Cohen and Turnbull,[3] who maintain that diffusing particles are confined most of the time to cages bounded by their immediate neighbors. A cage may enlarge due to density fluctuations thus permitting displacement of the particle. This displacement results in a net diffusive motion only when another particle enters the cage before the first can return to its initial position.

Our simulation model for spherical penetrants in a polymer matrix assumes that the cage for a penetrant is defined by the segment of a polymer chain contained in a sphere whose diameter is approximately one correlation length, i.e., a "blob".[4] Within each blob, the chain does not interact with other chains and excluded volume behavior is exhibited. The chain as a whole (a succession of blobs) is Gaussian and the effective interactions between blobs are weak. Because penetrant molecules at low concentration experience only a small fraction of the free volume (and, in any case, the segment density inside a blob is equivalent, on average, to the bulk density), the free volume inside a blob should be representative of the polymer free volume. In order to maintain mathematical tractability, the cage, or cavity of free volume, is required to lie on the midpoint of the blob's end-to-end vector. Also assumed is a theoretical expression for the probability distribution of cavity sizes, developed below. Lastly, the rotational isomeric state (RIS) approximation[5] was used.

Theoretical Considerations

In a polymer above but not too far removed from the glass transition temperature, the free volume is a small fraction of the total volume. At equilibrium, it is distributed in small, continuously varying amounts of all possible shapes so that $f(V)\,dV$ is the probability of finding a cavity of free volume between V and $V + dV$. Because these pockets of free volume are very dilute, the one-cavity distribution totally describes the free volume distribution. Also, we assume there are no energetic interactions between cavities; otherwise, coalescence of two cavities would result in a single, larger cavity to reduce surface-reversible work contributions. The total average free volume is fixed at equilibrium and given by $\bar{N}\langle V\rangle$ where $\bar{N}$ is the equilibrium mean number of cavities at temperature T and $\langle V\rangle$ is the mean volume per cavity.

In order for a small molecule to diffuse in the polymer, a minimal volume V_m must be available adjacent to the dissolved small molecule or penetrant. We assume that the shape correction is already included in the definition of V_m since not all cavities having a volume equal to or greater than that of the penetrant are of the right shape to hold a penetrant molecule.

Because the free volume is so dilutely dispersed and is described by $f(V)$, we can treat cavities as an ideal gases possessing a (one-particle) entropy S:

$$\frac{S}{k} = -\int_0^\infty [f(V)\ln f(V) - f(V)]\,dV \tag{2}$$

The distribution $f(V)$ must be normalized

$$\int_0^\infty f(V)\,dV = 1 \tag{3}$$

and must also be consistent with the given equilibrium mean free volume of a cavity, $\langle V\rangle$:

$$\langle V\rangle = \int_0^\infty f(F)V\,dV \tag{4}$$

Optimizing S with respect to all variations δf in f, using Lagrange multipliers, yields

$$f(V) = \frac{e^{-V/\langle V\rangle}}{\langle V\rangle} \tag{5}$$

The probability of finding a cavity with free volume greater than or equal to V_m adjacent to a penetrant is given by

$$P(V \geq V_m) = \int_{V_m}^\infty f(V)\,dV = e^{-V_m/\langle V\rangle} = e^{-(\bar{N}V_m/V_t)/f(T,\varphi)} = e^{-B/f(T,\varphi)} \tag{6}$$

where V_t is the total volume of the system, $B = \rho V_m$, ρ being the number density of cavities, and the free volume fraction $f(T,\phi)$ is given by

$$f(T,\phi) = \bar{N}\langle V\rangle / V_t \tag{7}$$

Equation 6 resembles the equation derived by Cohen and Turnbull[3] by assuming a lattice model in which the free volume is an integral number of lattice vacancies. Besides freeing the derivation from the lattice constraint (after all, polymers *are* amorphous), the present approach yields the correctly normalized B for the off-lattice chains.

The usual free volume models[1,3] for diffusion set D proportional to $P(V \geq V_m)$, yielding eq 1. Currently, theory does not evaluate $f(T,\phi)$, ρ, or A in molecular terms. These ideas can, however, be used, together with the notion that a polymer melt (like a very concentrated solution) is essentially a closely packed system of blobs,[4] to construct a simulation model from which $f(T,\phi)$ can be evaluated.

The Monte Carlo Simulation Model

In order to predict reliable structure-property relationships of polymers, a model must specifically account for chemical structure. Our model[6] uses geometric and statistical information for a particular chain through the RIS approximation[5] to produce Monte Carlo generated conformations of short segments of the macromolecule. The segment length corresponds to the average chain distance between intermolecular contacts, i.e., portions of the chain that form individual blobs.

The chain length associated with a blob can be inferred from the empirical findings of Fox et al.,[7] whose viscosity studies suggest that chain domains fail to overlap to some critical extent for polymers with less than 600 chain atoms. This value is viewed as an upper limit because scaling theory[4] shows that the correlation length is proportional to the $-3/4$ power of concentration and, therefore, the number of monomers per blob decreases even more rapidly, with the $-5/4$ power of concentration. Unfortunately, proportionality constants for these scaling relationships are not known, preventing calculation of the number of monomers per blob at a given concentration. Values of 10, 15, 20, and 25 were chosen for the degrees of polymerization of the chain segments used for the simulations.

A spherical cavity of free volume is assumed to exist on the midpoint of the segment's end-to-end vector (see Figure 1). After van der Waals radii were placed on the chain constituents, the size of the cavity is determined. Repeating this process for a statistically representative population (10,000) of chain segments allows evaluation of the probability $P(r \geq r_m)$ of a chain having a cavity with a radius greater than or equal to a given value. Given the constraints of the model, this is equivalent to $P(V \geq V_m)$ in eq 6.

A standard Monte Carlo technique[8-14] based on the RIS approximation was used to generate chain confor-

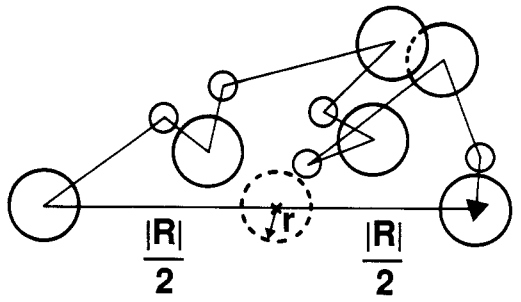

Figure 1. Schematic depiction of a spherical cavity centered on the midpoint of the end-to-end vector of a hypothetical chain. A relatively low value (6) of the degree of polymerization was chosen for purposes of clarity.

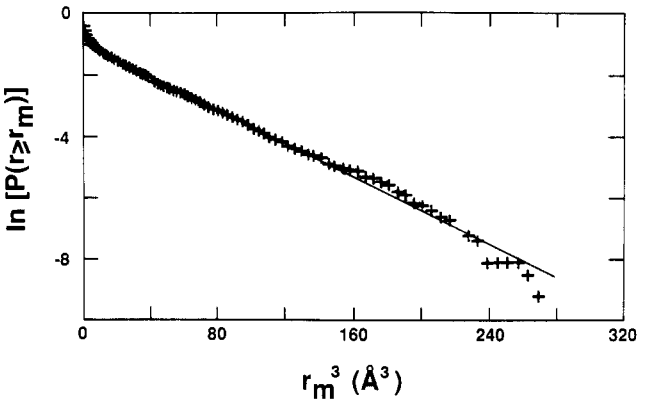

Figure 2. ln $P(r \geq r_m)$ versus r_m^3 for PDMS with DP = 20. Data points (+) are from the simulation and the solid line was drawn from a least-squares fit to the data, ignoring $r_m^3 \leq 0.5$ Å^3.

mations with a specified degree of polymerization (DP). For poly(dimethylsiloxane) (PDMS), the structure and conformational information needed for the RIS analysis were obtained from previous experimental and theoretical investigations.[8,14] The Si–O bond length is 0.164 nm, and the Si–O–Si and O–Si–O bond angle supplements are 37° and 70°, respectively. For purposes of illustration, some calculations were done with both bond angle supplements arbitrarily set to 70°.[6] The rotational states are located at ϕ = 0° or trans, ϕ = 120° or gauche$^+$, and ϕ = −120°, or gauche$^-$. The chain statistics for (atactic) poly(methylpropylsiloxane) (PMPrS) are different than those for PDMS due to the larger pendant group. To account for this difference the method of Flory, Mark, and Abe was employed.[15] All simulations were performed for a temperature of 300 K.

Preliminary studies showed that the distribution of cavity sizes displayed little variation with the stereochemical placements in either an isotactic, a syndiotactic, or an atactic sense. The results presented below are therefore for atactic PMPrS only. Because the ring-opening polymerization process that produces PMPrS shows no preference for meso or racemic placements, a value of meso replication probability of 0.5 was assumed for Monte Carlo generation of these chains.

Analysis and Results

As seen in Figure 2, ln $P(r \geq r_m)$ is a linear function of r_m^3 for values of $r_m^3 > 0.5$ Å^3. It was interesting to note that arbitrarily making both bond angles of a chain equal decreased the probability of a given hole size.[6] This suggests that the significant differences in bond angles and the associated peculiarly curved trajectories[5,16] actually occurring in siloxane polymers could be an origin of packing inefficiencies and thus increased free volumes. For this model the number density ρ of free volume cavities is unity so all that is required to obtain the free volume fraction $f(T,\phi)$ is a value for the system volume V_t. It is reasonable to take this to be the volume of a sphere with radius equivalent to the radius of gyration of the chain segment averaged over all generated conformations.

Table I
Free Volume Fractions for Poly(dimethylsiloxane) (PDMS) and Poly(methylpropylsiloxane) (PMPrS)

DP[a]	PDMS	PMPrS
10	0.0746	0.0610
15	0.0885	0.0622
20	0.118	0.0895
25	0.129	0.109

[a] Degree of polymerization.

Free volume fractions for PDMS and PMPrS were calculated from linear least-squares fits to the data (with $r_m^3 \leq 0.5$ Å^3 neglected) for DP = 10, 15, 20, and 25. The results are presented in Table I. Notice that for a given polymer $f(T,\phi)$ increases with increasing DP. Since DP corresponds to chain length between intermolecular contacts, a larger DP corresponds to a less dense polymer matrix in this respect.

Also, for a given DP, PDMS has a significantly larger free volume than PMPrS. The effect on the diffusion coefficients can be crudely estimated by noting that D is proportional to $\exp[-B/f(T,\phi)]$ and assuming that both proportionality factors are the same and that both values of B are the order of unity. With the exception of DP = 15, the results suggest that D for PDMS should exceed that for PMPrS by a factor approximately ranging from 4 to 20. For DP = 15, this factor is 120. At 35 °C, the mutual diffusion coefficients for CO_2, CH_4, and C_3H_8 in PDMS exceed those in PMPrS by factors of 2.5, 3.2, and 3.7, respectively. Thus, the calculated results are in semiquantitative agreement with experiment. Given the limitations of our treatment, for example, the neglect of the effect of adjacent chains on the cavity size, the results are quite encouraging.

Acknowledgment. It is a pleasure to acknowledge the financial support provided J.E.M. by the Gas Research Institute through Grant No. 5082-260-0666 and to thank Dr. Andrzej Kloczkowski for his very helpful comments.

References and Notes

(1) Stern, S. A.; Frisch, H. L. *Annu. Rev. Mater. Sci.* **1981**, *11*, 523.
(2) Fujita, H. *Fortschr. Hochpolym. Forsch.* **1961**, *3*, 1.
(3) Cohen, M. H.; Turnbull, D. *J. Chem. Phys.* **1959**, *31*, 1164.
(4) de Gennes, P. G. *Scaling Concepts in Polymer Physics*; Cornell University Press: Ithaca, NY, 1979.
(5) Flory, P. J. *Statistical Mechanics of Chain Molecules*; Wiley-Interscience: New York, 1969.
(6) Lee, C.-L.; Stern, S. A.; Mark, J. E.; Hoffman, E. Final Report (GRI-87/0037), Investigation of Structure-Permeability Relationships of Silicone Polymer Membranes; Gas Research Institute: Chicago, IL, 1987.
(7) Fox, T. G.; Gratch, S.; Loshack, S. In *Rheology-Theory and Applications, Volume 1*, Eirich, F. R., Ed.; Academic Press: New York, 1956; Chapter 12.
(8) DeBolt, L. C.; Mark, J. E. *Macromolecules* **1987**, *20*, 2369.
(9) Yoon, D. Y.; Flory, P. J. *J. Chem. Phys.* **1974**, *61*, 5366.
(10) Flory, P. J.; Chang, V. W. C. *Macromolecules* **1976**, *9*, 33.
(11) Conrad, J. C.; Flory, P. J. *Macromolecules* **1976**, *9*, 41.
(12) Bruns, W.; Motoc, I.; O'Driscoll, K. F. *Monte Carlo Applications in Polymer Science*; Springer-Verlag: Berlin, 1980.
(13) Mark, J. E.; DeBolt, L. C.; Curro, J. G. *Macromolecules* **1986**, *19*, 491.
(14) Mark, J. E.; Curro, J. G. *J. Chem. Phys.* **1983**, *79*, 5705.

(15) Flory, P. J.; Mark, J. E.; Abe, A. J. Am. Chem. Soc. 1966, 88, 639.
(16) Mark, J. E. J. Chem. Phys. 1968, 49, 1398.
(17) Stern, S. A.; Shah, V. M. and Hardy, B. J. J. Polym. Sci., Polym. Phys. Ed. 1987, 25, 1263.

Registry No. CO_2, 124-38-9; CH_4, 74-82-8; C_3H_8, 74-98-6.

Molecular Weight and Comparative Studies of Poly-3- and Poly-4-BCMU Monolayers and Multilayers

J. E. Biegajski, R. Burzynski, D. A. Cadenhead,* and P. N. Prasad*

Department of Chemistry, State University of New York at Buffalo, Buffalo, New York 14214. *Received January 10, 1989; Revised Manuscript Received July 13, 1989*

ABSTRACT: The molecular weights of three poly-4-BCMU samples were determined with a film balance technique by assuming near ideal behavior at low film concentrations. For the high, medium, and low molecular weight samples the number-average molecular weights were 410 000, 300 000, and 66 000 g/mol, respectively. All three samples showed a monolayer/bilayer, yellow coil/red rod conformational change similar to those we previously reported;[1] however, the low molecular weight sample initiated the compressional transition at a significantly lower area/residue than did either the medium or high molecular weight samples. This was interpreted to mean that the shorter chains in the low molecular weight sample had an increased number of semisoluble end groups. The visible absorption spectra indicated that while the low molecular weight sample underwent a yellow coil/red rod transition more readily and to a greater extent, the resultant red rod form was somewhat less organized. We have also made further comparisons of poly-3- and poly-4-BCMU. A reevaluation of the thermodynamics of the monolayer/bilayer transition, as indicated by surface pressure/area per residue isotherms, using a modified Clapeyron equation, showed slight exothermicity and increasing order accompanying multilayer formation of red rod poly-4-BCMU. Resonance-enhanced, laser Raman spectroscopy clearly reveals that the upper layer of the condensed bilayer consists of the red rod form but that the residual lower layer remains in the yellow coil form. Transmission electron microscopy of both poly-3-BCMU and poly-4-BCMU reveals a transition from a smooth surface in the monolayer region to one exhibiting numerous rodlike features in the transition region until in the condensed phase a more uniform but textured appearance is achieved. The effects of both solid and aqueous substrates were also examined. Deposition of monolayers of both polymers on hydrophobic solid substrates gave clear visible spectroscopic evidence of a small, partially induced coil to rod transition, in contrast to similar monolayers deposited on hydrophilic solid surfaces. Changing the pH and the addition of both sodium and calcium ions to an aqueous substrate also had significant effects. For poly-4-BCMU high pH (12.5) values resulted in an overall expansion for both expanded and condensed isotherm segments. For poly-3-BCMU the condensed state was expanded but the expanded (monolayer) state was condensed. A combination of ionization and hydrolysis was invoked for both polymers with ionization predominating for poly-4-BCMU and hydrolysis playing a more significant role for poly-3-BCMU. Calcium ions were shown to greatly condense ionized films while high concentrations of sodium ions produced expansion. The latter resulted in nearly identical compressional isotherms for poly-3-BCMU and poly-4-BCMU, except for a shift of the highly sensitive transition region.

Introduction

Previously we have demonstrated that monolayers of both poly-4-BCMU[1] [poly(dibutyl 4,19-dioxo-5,18-dioxa-3,20-diaza-10,12-docosadiynedioate)] and poly-3-BCMU[2] [poly(dibutyl 4,17-dioxo-5,16-dioxa-3,18-diaza-9,11-eicosadiynedioate)] have surface pressure (π)–area per residue (A) isotherms exhibiting a phase transition that incorporates an intramolecular conformational transition from an expanded monomolecular amphipathic yellow coil form to a condensed multimolecular nonamphipathic red or blue rod form. The conformational transition, from coil to rod, has been previously reported, both in solution and solid-state films by others[3-8] and has been interpreted as representing an increased effective π-electron conjugation length along the polymer backbone. The transition is brought about either by changing the solvent toward a more nonpolar composition or by decreasing the temperature. This allows intramolecular hydrogen bonding to take place between adjacent side groups of the same polymer chain.

In this paper we report and compare the monomolecular film behavior of high and low molecular weight (MW) poly-4-BCMU samples. We will see that these show similar but somewhat different behavior from that of a medium MW poly-4-BCMU[1] through both π–A isotherms at the air/water interface and visible absorption spectra of Langmuir–Blodgett (LB) transferred films.

The number-average molecular weights of high, low, and previously studied medium MW samples of poly-4-BCMU were determined by using a film balance and a modified ideal gas law type equation, which applies at low surface pressures. π–A isotherms for medium MW poly-4-BCMU along with visible absorption spectra of LB transferred films are presented. Resonance Raman spectra of medium MW poly-4-BCMU transferred films provide complimentary evidence of the coil to rod conformational transition.

The relaxation observed between a continuous compression and a stepwise, "equilibrium" isotherm of poly-

* To whom correspondence should be addressed.

0024-9297/90/2223-0816$02.50/0